

Distinct MRI pattern in lesional and perilesional area after traumatic brain injury in rat – 11 months follow-up

Riikka J. Immonen^a, Irina Kharatishvili^b, Juha-Pekka Niskanen^a, Heidi Gröhn^c,
Asla Pitkänen^{b,d}, Olli H.J. Gröhn^{a,*}

^a Biomedical NMR research group, Biomedical Imaging Unit, Department of Neurobiology, A. I. Virtanen Institute for Molecular Sciences, University of Kuopio, P.O.B. 1627, FIN-70211 Kuopio, Finland

^b Epilepsy research group, Department of Neurobiology, A. I. Virtanen Institute for Molecular Sciences, University of Kuopio, P.O.B. 1627, FIN-70211 Kuopio, Finland

^c Department of Clinical Physiology, Nuclear Medicine and Neurophysiology, North Karelia central hospital, FIN-80120 Joensuu, Finland

^d Department of Neurology, Kuopio University Hospital, P.O.B 1777, FIN-70211 Kuopio, Finland

ARTICLE INFO

Article history:

Received 28 May 2008

Revised 29 August 2008

Accepted 8 September 2008

Available online 27 September 2008

ABSTRACT

To understand the dynamics of progressive brain damage after lateral fluid-percussion induced traumatic brain injury (TBI) in rat, which is the most widely used animal model of closed head TBI in humans, MRI follow-up of 11 months was performed. The evolution of tissue damage was quantified using MRI contrast parameters T_2 , $T_{1\rho}$, diffusion (D_{av}), and tissue atrophy in the focal cortical lesion and adjacent areas: the perifocal and contralateral cortex, and the ipsilateral and contralateral hippocampus. In the primary cortical lesion area, which undergoes remarkable irreversible pathologic changes, MRI alterations start at 3 h post-injury and continue to progress for up to 6 months. In more mildly affected perifocal and hippocampal regions, the robust alterations in T_2 , $T_{1\rho}$, and D_{av} at 3 h to 3 d post-injury normalize within the next 9–23 d, and thereafter, progressively increase for several weeks. The severity of damage in the perifocal and hippocampal areas 23 d post-injury appeared independent of the focal lesion volume. Magnetic resonance spectroscopy (MRS) performed at 5 and 10 months post-injury detected metabolic alterations in the ipsilateral hippocampus, suggesting ongoing neurodegeneration and inflammation. Our data show that TBI induced by lateral fluid-percussion injury triggers long-lasting alterations with region-dependent temporal profiles. Importantly, the temporal pattern in MRI parameters during the first 23 d post-injury can indicate the regions that will develop secondary damage. This information is valuable for targeting and timing interventions in studies aiming at alleviating or reversing the molecular and/or cellular cascades causing the delayed injury.

© 2008 Elsevier Inc. All rights reserved.

Introduction

Traumatic brain injury (TBI) is a prevalent cause of disability and mortality in industrialized countries (Leon-Carrion et al., 2005). After primary impact and injury, secondary injury develops over hours to months. It is composed of a complex and poorly understood combination of molecular, cellular (Karhunen et al., 2005), and metabolic (Kharatishvili et al., 2006) alterations in the central nervous system, which lead to post-injury functional disabilities including somatomotor impairment, cognitive decline, emotional disturbance, or epilepsy (Kharatishvili et al., 2006; Thompson et al., 2006). Many of the delayed pathological processes could potentially be reversed, thus they could provide targets for the development of recovery enhancing and/or antiepileptogenic treatments. To conquer this challenge, a non-invasive detection of the progression of pathology, which in particular can discern potentially reversible tissue damage from irreversibly

injured areas in individual subjects is critical for defining anatomic regions for application of such therapies

MRI is one of the most versatile imaging methods available today and provides an excellent tool to study the spatio-temporal progression of damage under controlled experimental settings. Currently, most of the experimental MRI studies of TBI have focused exclusively on the acute to subacute phase, that is, the time period extending from hours to days or a few weeks post-injury. Furthermore, the majority of the MRI follow-up studies report alterations in only one or two MRI contrast parameters such as volumetry of cortical atrophy, cortical edema related T_2 hyperintensity, and/or decreased apparent water diffusion (ADC) within hours after TBI followed by increased diffusion days or weeks after TBI (Albensi et al., 2000; Obenaus et al., 2007; Onyszchuk et al., 2007; Van Putten et al., 2005).

Nuclear magnetic resonance spectroscopy (MRS) has been used to assess metabolite changes during the acute and subacute phases after TBI. These studies have reported a decrease in *N*-acetylaspartate/creatinine ratio (NAA/Cr) and an increase in choline/creatinine (Cho/Cr) ratio in the lesion area and/or in the ipsilateral parietal cortex in

* Corresponding author. Fax: +358 17 16 3030.

E-mail address: olli.grohn@uku.fi (O.H.J. Gröhn).

rodents that have experienced fluid-percussion or controlled cortical impact injury (Berry et al., 1986; Choi et al., 2005; Schuhmann et al., 2002). Also, in the pericontusional zone Cr+PCr, NAA, and Glu were decreased from 1 h to 28 d post-injury (Dube et al., 2001) and persistently decreased in the combined hippocampus basal ganglia region up to 4 weeks after trauma (Schuhmann et al., 2002). However, there are no long-term studies available on changes in the metabolic profile after TBI.

The aim of this study was to investigate the spatio-temporal long-term progression of brain damage after TBI. We hypothesized that an MRI signature determined by multiparametric quantitative MRI can differentiate perilesional tissue from irreversibly damaged lesion. To test this hypothesis, we induced TBI using lateral fluid-percussion injury that is a clinically relevant rat model of closed head TBI in humans, then systematically quantified several relevant MRI contrast parameters for up to 11 months post-injury, including quantitative T_2 , $T_{1\rho}$, trace of the diffusion tensor (D_{av}), and volumetric changes. Furthermore, we evaluated chronic changes in the metabolic profile of the hippocampus by magnetic resonance spectroscopy (MRS).

Methods

The study design is summarized in Fig. 1. The Group 1 (14 rats with TBI and 4 with sham operation) was imaged at 3 h, 3 d, 9 d, 23 d, 2 months, 3 months and 6 months after TBI. In Group 2 (20 rats with TBI and 10 with sham operation), the imaging was started at 5 months to avoid the possible effects of repeated halothane anesthesia during early post-injury period on long-term progression of brain pathology. In addition, as data from Group 1 indicated, progression of some alterations was still ongoing at 6 months, and therefore, we decided to continue the observation period for up to 11 months in Group 2. We also added MR spectroscopy (MRS) into the study protocol of Group 2 to investigate the metabolic profile of chronic post-injury state. In addition to MRI follow-up data presented here, the severity of behavioural impairment at 9 months and seizure susceptibility at 12 months were tested before rats were sacrificed for histopathologic analysis. Some of these data have been presented previously ((Kharatishvili et al., 2007); behavioural data, manuscript in preparation).

Animal model

TBI was induced in adult male Harlan Sprague Dawley rats (total $n=48$, from which $n=34$ survived and were examined by MRI, 305–390 g; Harlan Netherlands B.V., Horst, the Netherlands) by lateral fluid-percussion brain injury as previously described (Kharatishvili et al., 2006; McIntosh et al., 1989). Animals were anesthetized with a mixture containing sodium pentobarbital (58 mg/kg), chloral hydrate

(60 mg/kg), magnesium sulfate (127.2 mg/kg), propylene glycol (42.8%), and absolute ethanol (11.6%), (i.p., 6 ml/kg). This anesthesia had been previously used in our laboratory in the same animal model with well described histopathological findings (Kharatishvili et al., 2006). The skull was exposed and a 5 mm diameter circular craniectomy was performed with a trephine between the bregma and the lambda on the left convexity (anterior edge 2.0 mm posterior to the bregma and the lateral edge adjacent to the left lateral ridge) leaving the dura intact. TBI was induced by a fluid-percussion device (AmScien Instruments, Richmond, Virginia, USA) with a brief (21–23 ms) transient pressure fluid pulse impact against the exposed dura. The pressures of the pulses were measured by a transducer extracranially. The force of the impact was adjusted to 2.6–3.3 atm to induce lateral FPI. Control animals had identical anesthetic and surgical operation without the impact ($n=14$).

During the follow-up period the animals were housed in individual cages and kept under controlled laboratory conditions (light regime of 12 h light/12 h dark, light on at 07:00 a.m.; temperature, 22 ± 1 °C; air humidity, 50–60%, *ad libitum* access to food and water).

All animal procedures were approved by the Committee for the Welfare of Laboratory Animals of the University of Kuopio and the Provincial Government of Kuopio, and conducted in accordance with the guidelines set by the European Community Council Directives 86/609/EEC.

Magnetic resonance imaging (MRI)

MRI data were acquired at a horizontal 4.7 T magnet (Magnex Scientific Ltd, Abington, UK) with actively shielded imaging gradients (Magnex) interfaced to a Varian (Palo Alto, CA) UNITYINOVA console and using a quadrature half-volume RF coil (diameter 28 mm/two 18 mm loops, HF Imaging LLC, Minneapolis, MN) in transmit/receive mode. Rats were anaesthetised with 1% halothane in N_2O/O_2 (70%/30%), securely fixed into a stereotactic holder and kept warm with a water circulating heating bed underneath the animals.

Volumetric changes were detected using a T_2 weighted spin echo multi-slice sequence with two adiabatic refocusing RF pulses to minimize the influence of moderately inhomogeneous B_1 field (echo time 70 ms, repetition time 3 s, field of view 30×30 mm² covered with 128×256 data points, slice thickness 0.75 mm, 19 consecutive slices covering rat cerebrum). T_2 , $T_{1\rho}$ and the 1/3 of the trace of diffusion tensor (D_{av} ; $D_{av}=1/3$ trace D) were quantified from the same single coronal slice (corresponding to the antero-posterior level of –3.80 mm from the bregma according to Paxinos rat brain atlas, Paxinos and Watson, 1986) using a magnetization prepared fast spin echo sequence with adiabatic BIR-4 refocusing pulses (repetition time 3.0 s, 16 echoes/excitation, center-out k -space filling, echo spacing 10 ms, field of view of 30×30 mm² covered with 128×256 data points,

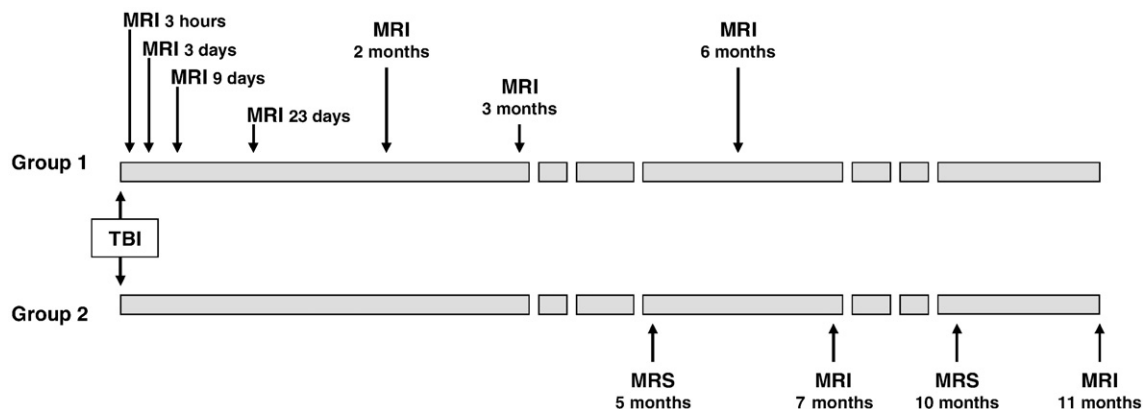


Fig. 1. Study design. After induction of traumatic brain injury (TBI) by lateral fluid-percussion, MRI was performed at 3 h, 3 d, 9 d, 23 d, 2 months, 3 months and 6 months in Group 1 (14 TBI, 4 controls) and at 7 months and 11 months post-injury in Group 2 (20 TBI, 10 controls). In Group 2, also MRS was performed at 5 months and 10 months after TBI.

slice thickness 1.50 mm). T_2 relaxation time was measured using a spin echo preparation block consisting of adiabatic half passage (AHP), two hyperbolic secant (HS) adiabatic full passages, reverse AHP and crusher gradient in front of the fast spin echo sequence (echo times (TE)=20, 38, 52, 76 ms). On-resonance longitudinal rotating frame ($T_{1\rho}$) relaxation time was measured using variable-length adiabatic spin lock preparation pulse consisting of three parts: AHP, continuous wave on-resonance spin lock period and reverse AHP pulse, (spin lock times (SL)=18, 38, 58, 78 ms, $B_{1SL}=0.8$ G) (Grohn et al., 2005) and crusher gradients were placed in front of the fast spin echo sequence. 1/3 of the trace of the diffusion tensor (D_{av}) was quantified using the same pulse sequence as in our T_2 measurement with a diffusion sensitising gradient pair positioned around each refocusing RF pulse in the magnetization preparation block. Three images with different degree of diffusion weighting ($b=90, 496, 1014$ s/mm², diffusion time=29 ms) were all obtained in three different orthogonal orientations: x, y and z . Data for B1 field map were acquired using variable-length square preparation pulse with a crusher gradient in front of a FLASH pulse sequence (TR=4.5 ms, TE=2.2 ms), and B1 maps were calculated by fitting a cosine function to the measured signal intensity oscillation.

MRI data analysis

The volumes of the lesion at all time points and of the hippocampus 6 months post-injury were calculated by manually outlining the regions of interest into the T_2 weighted multi-slice set covering the whole brain. We defined lesion volume as a combined volume of focal lesion and ipsilateral ventricle. This was because the distinction between the two regions was practically impossible at the later time points, when progressive destruction of cellular structures leads to complete tissue loss and the arising cavity is filled with cerebrospinal fluid. Quantitative T_2 and $T_{1\rho}$ relaxation times and diffusion maps were calculated from a 1.5 mm-thick single slice by fitting the data voxel wise to standard single exponential formulae in Matlab. The diffusion coefficient D was measured and calculated separately in three different orthogonal orientations (D_x, D_y and D_z) and the average of these three coefficients was determined as an orientation independent measure of water diffusion D_{av} . The analysis was performed using an in-house written program in Matlab 7.1 (MathWorks, Natick, MA). Five regions of interest (ROI) were manually drawn. The *focal area* refers to the lesioned cortex that was outlined based on hyperintensity in T_2 weighted images and using the visual aid of T_2 maps with scaling of 0–150 ms to standardize the analysis and more accurately detect the limit between hyperintense and healthy-appearing tissue (Fig. 2). *Perifocal area* refers to the ipsilateral parietal cortex (somatosensory and auditory cortex according to Paxinos' rat atlas) excluding the focal lesion and including tissue that appears normal in T_2 weighted images. In addition, we assessed the contralateral parietal cortex and the *hippocampus* bilaterally (Fig. 2).

When outlining the perifocal and hippocampal ROIs, the voxels overlapping with the enlarged ventricles were excluded to avoid partial volume effect, and to detect the possible degenerative process ongoing in the normal appearing tissue.

Magnetic resonance spectroscopy (MRS) measurements and analysis

The *in vivo* single voxel spectroscopy data were obtained using stimulated echo acquisition mode (STEAM) localization with short echo time (Tkac et al., 1999) (TE=2 ms, TR=4 s, bandwidth of 2.5 kHz was covered with 3336 points, averages=512) incorporating VAPOR water suppression scheme, after automatic FASTMAP shimming (Gruetter 1993). Voxels (2.5 mm*3 mm*3 mm) were placed in both the ipsilateral and contralateral hippocampus (Fig. 2). The spectral analysis was performed using LC model and only results from metabolites with SD%<20 were included in further analysis. All values are given as relative concentrations to total creatine peak at 3.04 ppm consisting of creatine and phosphocreatine.

Statistics

All values are indicated as mean±standard deviation (std). Statistical evaluation was performed using SPSS for Windows software (Chicago, IL, version 14.0). Differences between TBI and control groups were calculated using Kruskal–Wallis followed by *post hoc* analysis with Mann–Whitney U test (non-parametric tests used due to the low animal number). Differences between time points were calculated using Friedman followed by *post hoc* analysis with Wilcoxon test. $P<0.05$ was considered significant.

Results

Mortality (*death within 72 h post-injury*) in Group 1 was 25% and in Group 2 21% suggesting that in both groups the lateral fluid-percussion TBI was moderate in severity (Dubreuil et al., 2006; McIntosh et al., 1989; Thompson et al., 2005), and there was no difference between the Groups. Also the severity of impact as expressed in atm was similar (Group 1: range 2.3–3.2 atm, mean 2.64 atm; Group 2: range 3.0–3.1 atm, mean 2.86, no difference between groups).

Temporal progression of lesion volume

As in other laboratories (McIntosh et al., 1989; Smith et al., 1997), even though the injury-induction parameters were similar from animal to animal, we found substantial variability in the severity of cortical lesion between individual animals. The variation in the lesion size can be described by categorizing the rats in Group 1 into the three subgroups based on T_2 weighted images acquired at 23 d post-injury

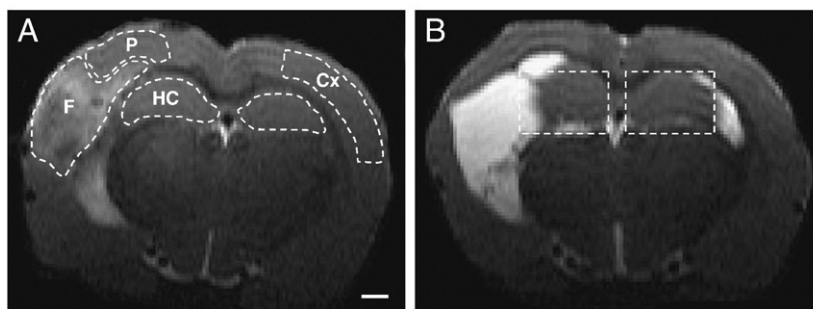


Fig. 2. (A) ROIs (dashed lines) drawn on a T_2 weighted image acquired at 3 d post-injury showing the location of injury-induced focal lesion (F), perifocal area (P), contralateral cortex (Cx), and hippocampus (HC). (B) A T_2 weighted image acquired 11 months post-injury showing the location of MRS voxels (dashed square, $3.0 \times 2.5 \times 3.0$ mm³) in the ipsilateral and contralateral hippocampus. Scale bar equals 1 mm.

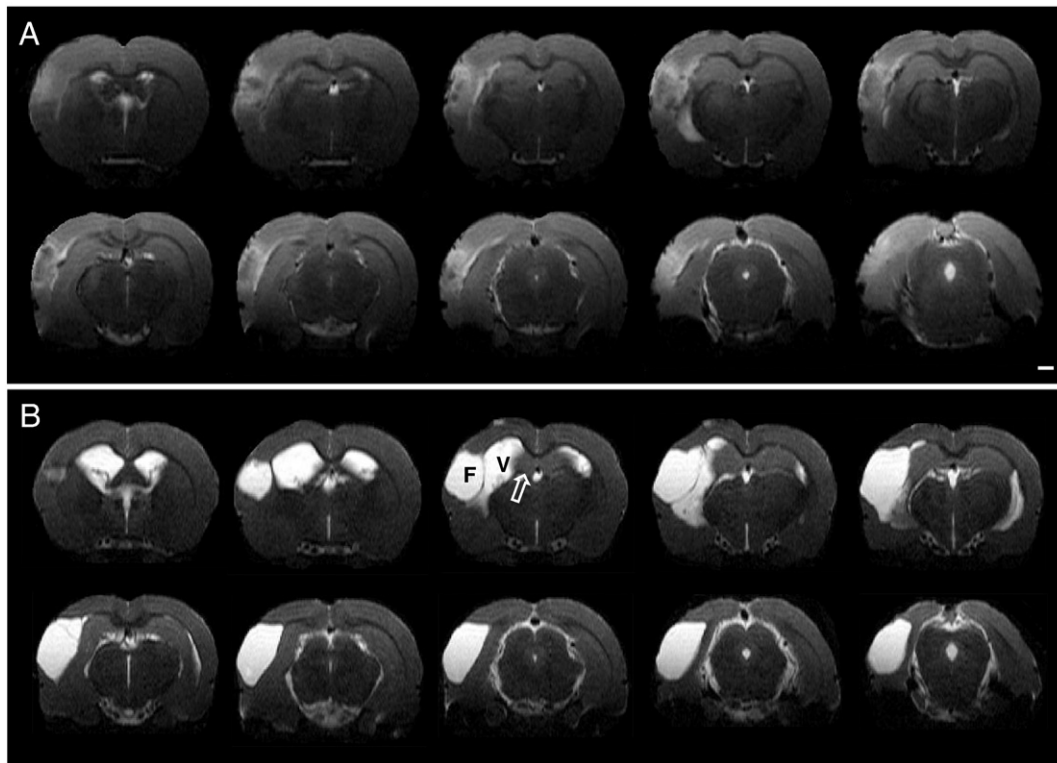


Fig. 3. Rostro-caudal extent of the focal lesion in coronal T_2 weighted multi-slice images acquired (A) at 3 d post TBI and (B) 6 months post TBI. Images in A and B are from the same representative animal. Note the extension of focal lesion (F), enlargement of ipsilateral ventricle (V), and decrease of hippocampal volume (arrowhead) over 6 months follow-up. Scale bar equals 1.5 mm.

when lesion outlines were most clearly visible (as compared to the earlier time points when oedema caused the lesion edges to appear blurred). Five of 14 animals had “mild” lesion that extended through maximum 5 MRI slices (rostro-caudal extent 0.75–3.75 mm) and had a volume $< 11 \text{ mm}^3$ at 23 d and volume $< 11.6 \text{ mm}^3$ for the whole follow-up period (the “mild” group includes one rat with no detectable

lesion). Six of 14 rats had “moderate” lesion that was detected in 5–11 slices (rostro-caudal extent 3.75–8.25 mm) and had a volume between 11–30 mm^3 which increased further after day 23. The remaining 3 of the 14 animals had the most severe lesions with volume $> 30 \text{ mm}^3$ that extended over 12–14 slices (rostro-caudal extent 9.0–10.5 mm; an example of a severe lesion is shown in Fig. 3).

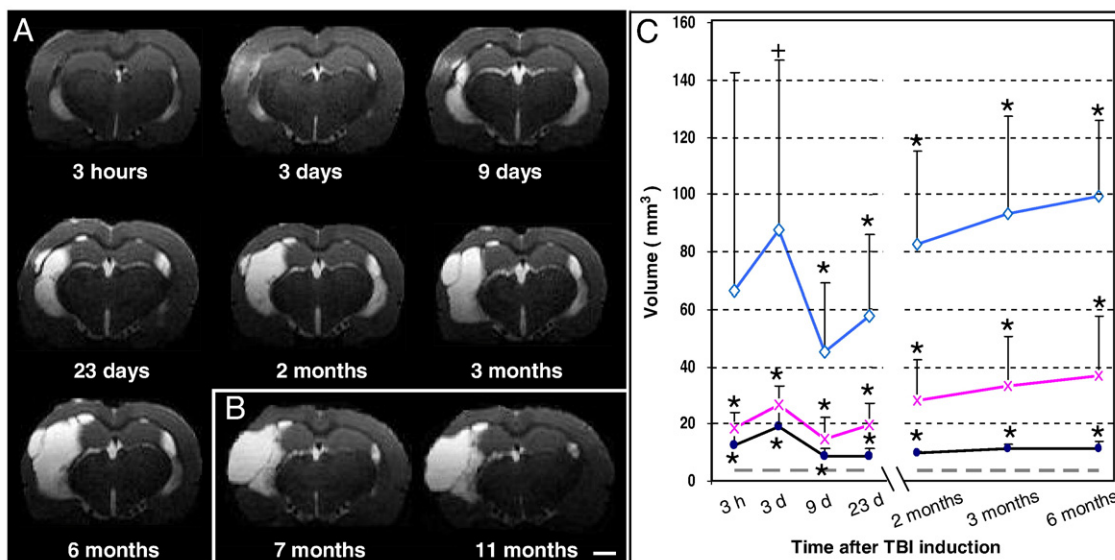


Fig. 4. Temporal progression of lesion volume in T_2 -weighted images. (A) Coronal slices from a representative animal in Group 1 acquired from the center of the lesion at different follow-up points demonstrating the progressive increase in focal lesion volume. Note also a decrease in the cross-sectional area of the ipsilateral hippocampus. (B) Coronal images from a rat in Group 2 acquired at 7 and 11 months post-injury. (C) Development of lesion volume (i.e., combined volume of the focal lesion and the ipsilateral ventricle) in mild, moderate and severe subgroups of Group 1 during 6 months follow-up post-injury. The dotted horizontal gray line is the baseline, i.e. the mean \pm std ($= 3.6 \text{ mm}^3$) of the ipsilateral ventricle volume of sham-operated controls. Group average data are shown as mean \pm std. Statistical differences: * $p < 0.01$ and $+p < 0.05$ as compared to sham-operated controls (Kruskall–Wallis with Mann–Whitney *post hoc* test). Scale bar in panels A and B equals 1.5 mm.

Fig. 3 demonstrates the rostro-caudal extent and progression of tissue atrophy in the same injured animal at 3 d and 6 months post-injury. Following TBI, the lesion formation and the progression of atrophy were evident from the increasing size of cortical lesion, enlargement of the ipsilateral ventricle, and decreasing size of the ipsilateral hippocampus.

Analysis of the temporal progression of lesion volume (i.e., combined volume of the focal cortical lesion and the ipsilateral ventricle in slices, in which focal cortical lesion is visible) is presented in Fig. 4. As is apparent in a representative case shown in Fig. 4A, lesion in T_2 weighted images at 3 d post-injury appeared larger and more hyperintense than at 3 h. The volume of the hyperintense region was reduced at 9 d as compared to the 3 d time point probably reflecting the resolution of vasogenic edema. It should be noted that the temporal profile of lesion volume development was similar in all animals despite large variation in the lesion size between individual animals (Fig. 4C).

Quantitative analysis (Fig. 4C) indicated that in Group 1, the lesion volume increased for 3 months ($p < 0.01$ as compared to the previous follow-up point within the same group 23 d, 2 months, and 3 months

post-injury, Friedman with Wilcoxon *post hoc* test). The further increase from 3 to 6 months was not statistically significant ($p = 0.055$). In line with these data, MRI volumetry in Group 2 did not reveal any increase in the lesion volume at the chronic stage (lesion volume at 7 months vs. 11 months, Figs. 4B and C).

The hippocampal volume was analyzed 6 months after the injury and the ipsilateral hippocampus showed volume decrease of 21% as compared to the controls (TBIs: 25.3 ± 2.9 mm³, controls: 32.0 ± 1.2 mm³, $p < 0.01$). The contralateral hippocampus did not display any volume loss.

Temporal pattern of changes in quantitative MRI contrast parameters is region-dependent

Diffusion (D_{av})

Diffusion (D_{av}) changes during the 11 months follow-up are summarized in Fig. 5. In the area of focal lesion, 3 of 14 animals with TBI showed acute diffusion drop of around 10% at 3 h post-injury (compare the data in the perifocal area and the ipsilateral

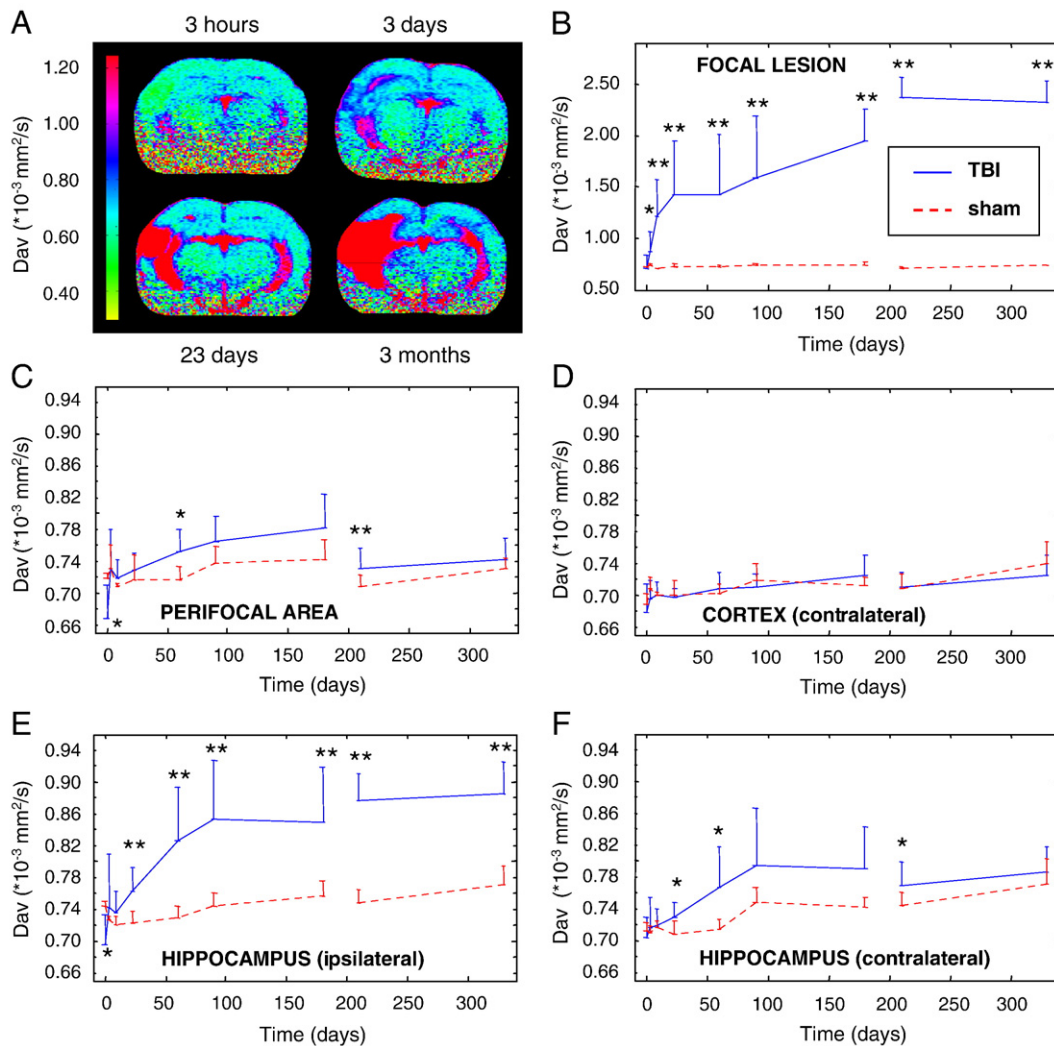


Fig. 5. Diffusion of water (D_{av}) in different brain areas over time after the induction of TBI. (A) D_{av} maps of a representative animal at four different time points after the TBI. Panels B–F show the progression of D_{av} in different regions during 11 months follow-up (Group 1: imaging at 3 h, 3 d, 9 d, 23 d, 2 months, 3 months and 6 months post-injury; Group 2: imaging at 7 and 11 months post-injury). Note a rapid increase in D_{av} in focal cortical lesion starting at 3 d post-injury (B). In the perifocal area and the ipsilateral hippocampus, diffusion decreases at 3 h post-injury with continuous increase thereafter being back to control values at 3–9 d post-injury (C and E). Interestingly, while the contralateral cortex does not show any changes (D), a delayed increase of D_{av} is detected in contralateral hippocampus (F). Data are shown as \pm std. Statistical significances: * $p < 0.05$; ** $p < 0.01$ as compared to sham-operated controls (Kruskal–Wallis with Mann–Whitney *post hoc* test). Data of panel E have been presented previously (Kharatishvili et al., 2007). Note the different y-axis range in primary lesion (panel B) than in other regions (panels C–F).

hippocampus). Starting at 3 d post-injury, D_{av} increased dramatically indicating loss of diffusion limiting structures, that is, ongoing tissue loss. At 3 d post-injury, D_{av} values were 19%, at 9 d 70%, at 23 d 99%, and at 6 months 120% higher than those in controls. In Group 2 at 7 to 11 months post-injury, the D_{av} was 218–240% of that in controls. The progressive D_{av} increase indicated that the tissue degradation in the focal lesion continues for several months post-injury. There was no further increase of D_{av} from 7 months to 11 months post-injury (Fig. 5B).

In the *perifocal area* D_{av} showed a modest acute drop of 7% ($0.05 \times 10^{-3} \text{ mm}^2/\text{s}$) at 3 h post-injury ($p < 0.05$ compared to controls, Fig. 5C). Thereafter, D_{av} returned to normal, and later showed a trend towards increased values throughout the entire follow-up period [increase as compared to controls at 2 months post-injury was 5% ($p < 0.05$) and at 7 months 3% ($p < 0.01$)].

Like in the adjacent perifocal area, also in the *ipsilateral hippocampus* the D_{av} showed an acute drop of 6% ($0.04 \times 10^{-3} \text{ mm}^2/\text{s}$, $p < 0.05$) at 3 h post-injury as compared to controls (Fig. 5E). D_{av} returned to normal during the next 3–9 d, and thereafter, started to increase being at 23 d

post-injury elevated by 7% ($p < 0.01$) as compared to controls. The progression continued for 3 months, when D_{av} was 15% higher than controls ($p < 0.01$). Thereafter, the increase levelled off and D_{av} remained elevated throughout the rest of the 11-months follow-up (the plateau of the final increase was 15–17% above the control level, $p < 0.01$). (Fig. 5E)

There was no initial drop in D_{av} in the *contralateral hippocampus*. A secondary increase in D_{av} was noticed starting 23 d post-injury when D_{av} was 3% higher than that in controls ($p < 0.05$). Increase in D_{av} continued for the next month finally leaving D_{av} 8% elevated. Thereafter, no further increase was detected (Fig. 5F). There were no changes in the D_{av} in the *contralateral cortex*.

T_2 and $T_{1\rho}$ relaxation times

The changes in T_2 and $T_{1\rho}$ are summarized in Figs. 6 and 7. The pattern of changes in these parameters during the 11 months follow-up resembled each other, so are therefore described together. At 3 h post-injury, the absolute T_2 in the focal lesion did not statistically differ from that in controls even though in most of the injured animals

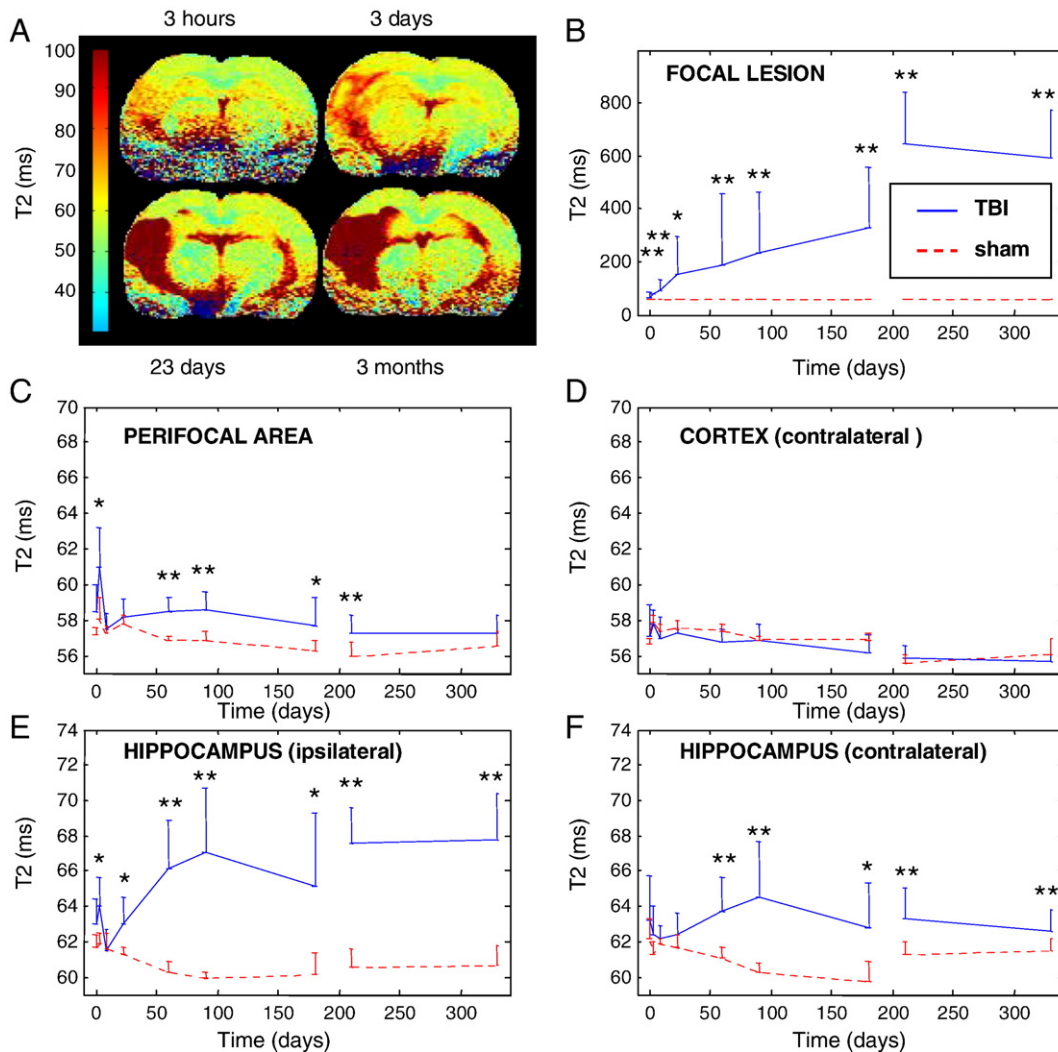


Fig. 6. T_2 in different brain areas over time after the induction of TBI. (A) The T_2 maps of a representative animal at different time points. Panels B–F show the progression of T_2 in different regions during 11 months follow-up (Group 1: imaging at 3 h, 3 d, 9 d, 23 d, 2 months, 3 months and 6 months post TBI, and Group 2: imaging at 7 and 11 months post TBI). In focal cortical lesion T_2 starts to increase at day 3 post-injury (B). The perifocal area (C) and the ipsilateral hippocampus (E) show a peak in T_2 at 3 d post-injury, recovery thereafter, and then, a secondary increase. In the ipsilateral hippocampus the secondary increase is substantially more pronounced than in the perifocal area. No changes were detected in the contralateral cortex (D), whereas the contralateral hippocampus shows a clear delayed increase in T_2 at 2 months onwards (F). Data are shown as mean \pm std. Statistical significances: * $p < 0.05$; ** $p < 0.01$ as compared to sham-operated controls (Kruskal–Wallis with Mann–Whitney *post hoc* test). A part of the data of panel E has been presented previously (Kharatishvili et al., 2007). Note the different y-axis range in primary lesion (panel B) than in other regions (panels C–F), and that the range of y-axis of C and D as compared to E and F have been shifted according to the level of control values.

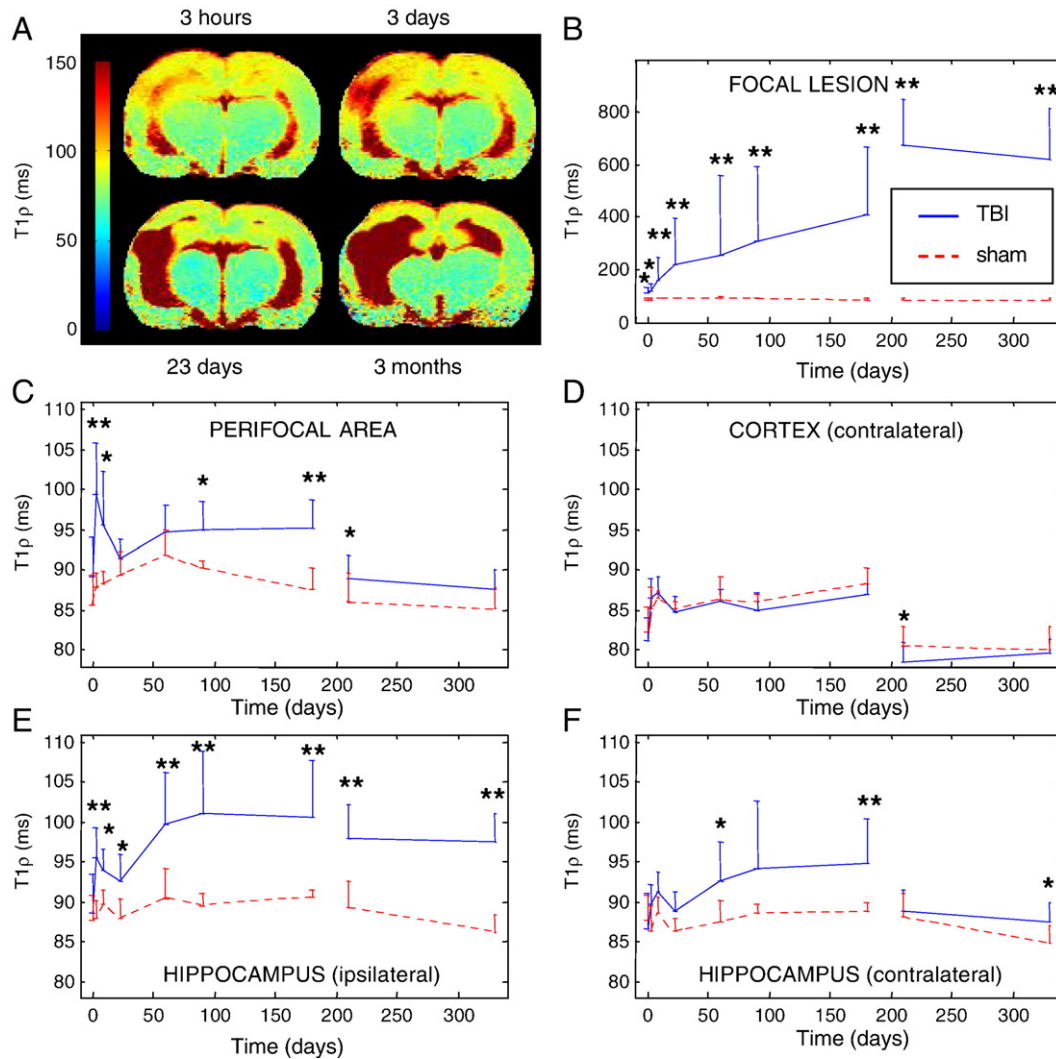


Fig. 7. $T_{1\rho}$ in different brain areas over time after the induction of TBI. (A) The $T_{1\rho}$ maps of a representative animal at four time points post-injury. Panels B–F show the progression of $T_{1\rho}$ during 11 months follow-up in different regions (Group 1: imaging at 3 h, 3 d, 9 d, 23 d, 2 months, 3 months and 6 months post-injury; Group 2: imaging at 7 and 11 months post-injury). Note that in focal cortical lesion (B) $T_{1\rho}$ increases immediately at 3 h post-injury and does not recover during the 11 months follow-up. Also in the ipsilateral hippocampus (E) there is peak at 3 d that shows a decrease towards control values at 9 d post-injury before starting a delayed increase lasting for the next month. Like in D_{av} and T_2 , there is a delayed increase in $T_{1\rho}$ in the contralateral hippocampus at 2 months onwards (F). Data are shown as mean \pm std. Statistical significances: * $p < 0.05$; ** $p < 0.01$ as compared to sham-operated controls (Kruskall–Wallis with Mann–Whitney *post hoc* test). Note different y-axis range in primary lesion. In all the other areas the same y-axis range is used allowing direct comparison of the changes. Note also that the difference in $T_{1\rho}$ between controls in Group 1 and Group 2 is due to the differences in B_1 values. Rats in Group 2 were older with larger heads which did not allow the half-volume RF coil to be placed to the same distance from ROIs as at 6 months. This increased distance lowered the B_1 field by 10% in the perifocal area, 11% ipsilateral hippocampus, 14% in the contralateral hippocampus, and 14% in the contralateral cortex in Group 2 as compared to Group 1. As $T_{1\rho}$ depends directly on B_1 (Grohn et al., 2000) the decrease in B_1 values explains the corresponding decrease in $T_{1\rho}$ values (for example, in the contralateral cortex the B_1 is 14% lower in Group 2 as compared to Group 1, and the $T_{1\rho}$ decrease is 10%).

we could observe a hyperintense lesion in T_2 -weighted signal intensity images (Fig. 4A). Starting on day 3, T_2 showed prolongation ($T_2 = 17$ ms, 29% higher than in controls, $p < 0.01$, Fig. 6B) and it continued to increase throughout the 6-months follow-up. Unlike T_2 , $T_{1\rho}$ was already prolonged at 3 h post-injury (23 ms, i.e., 27% as compared to controls, $p < 0.01$), and increase in the duration of $T_{1\rho}$ progressed similarly as in T_2 during the 6 months follow-up (Fig. 7B). There was no further increase in T_2 or $T_{1\rho}$ in the focal lesion area from 7 to 11 months after TBI.

In the perifocal area T_2 and $T_{1\rho}$ remained at control level at 3 h post-injury. Thereafter, both relaxation times showed a marked increase at 3 d post-injury as compared to controls [$T_{1\rho}$ increased by 12 ms (13%, $p < 0.01$) and T_2 by 3 ms (5%, $p < 0.05$)]. At 9 d post-injury, T_2 had recovered to the control level while $T_{1\rho}$ still remained elevated [7 ms, (8%, $p < 0.05$ as compared to controls)]. A trend of secondary increase in both T_2 and $T_{1\rho}$ was detected on day 23 that became significant at 2

(T_2) or 3 ($T_{1\rho}$) months post-injury as compared to controls. Thereafter, neither the T_2 nor $T_{1\rho}$ displayed any further increase but both remained elevated as compared to controls ($T_{1\rho}$ by 3–9% and T_2 by 2–3%, see Figs. 6C and 7C).

Also in the ipsilateral hippocampus the T_2 and $T_{1\rho}$ remained at control level at 3 h post-injury. Thereafter, both relaxation times showed a significant increase at 3 d post-injury [T_2 increased by 2 ms (3%, $p < 0.05$) and $T_{1\rho}$ by 8 ms (9%, $p < 0.01$) as compared to controls]. Similar to the perifocal area, at 9 d after TBI T_2 had recovered to the control level while $T_{1\rho}$ remained elevated [4 ms (5%, $p < 0.05$ as compared to controls)]. On day 23, both T_2 and $T_{1\rho}$ were elevated as compared to controls [T_2 1 ms (3%, $p < 0.05$) and $T_{1\rho}$ 5 ms (5%, $p < 0.05$), Figs. 6E and 7E]. From 23 d to 2 months, both T_2 and $T_{1\rho}$ showed a remarkable secondary increase (both $p < 0.01$) and became elevated by 6 ms (10%, $p < 0.01$) and 9 ms (10%, $p < 0.01$), respectively, as compared to controls. Between 2 to 6 months neither relaxation showed further

increase but both remained elevated as compared to controls ($T_{1\rho}$ by 10–13% and T_2 by 8–12%). Taken together, the observed changes were more pronounced in the ipsilateral hippocampus than in the perifocal area.

In the contralateral hippocampus the changes in the T_2 and $T_{1\rho}$ relaxation times followed a similar temporal profile as in the ipsilateral hippocampus but the magnitude of changes was substantially milder. Importantly, the occurrence of secondary damage was detected also in the contralateral hippocampus as increased T_2 and $T_{1\rho}$ at 2 months post TBI [T_2 increase was 3 ms (4%, $p < 0.01$) and $T_{1\rho}$ increase 5 ms (6%, $p < 0.05$) as compared to controls]. Also in the contralateral hippocampus, the relaxation times remained elevated throughout the 11 months follow-up (Figs. 6F and 7F).

Volume of the primary focal lesion did not correlate with the severity of damage in the perifocal areas

To find out if there is potentially viable perifocal tissue in the animals with very large focal lesions we studied the relationship between primary focal lesion volume and the severity of damage in more distal perifocal and hippocampal areas. Fig. 8 clearly shows the absence of any correlations, that is, the severity of the pathological change in MRI contrast parameters (i.e. the increase of T_2 , $T_{1\rho}$ and D_{av})

within the perifocal area outside the primary focal lesion did not depend on the size of the primary focal lesion. The analysis was performed at the particularly interesting time point of 23 d post-injury when the transient oedema no longer dominates the MRI findings, and the secondary injury cascades in the perifocal areas have begun, but there is still time for potential interventions if the tissue at risk can be identified. Importantly, this indicates that the lesion size alone does not describe the overall 'injury severity' and, in particular, lesion size does not describe the viability of perilesional regions. In several cases in spite of the large volume of the focal lesion (inside of which irreversible tissue damage is indicated by the magnitude of MRI contrast parameter changes) there were only small changes in MRI contrast parameters in the perifocal and hippocampal areas.

Chronic metabolic abnormalities as revealed by hippocampal MR spectroscopy

Five months post-injury we found decreased relative concentrations (relative to total Cr consisting of Cr+PCr) of γ -aminobutyric acid (GABA), glutamate (Glu), *N*-acetylaspartylglutamate (NAAG), *N*-acetylaspartate + *N*-acetylaspartylglutamate (NAA+NAAG) and glutamate + glutamine (Glu+Gln) in the ipsilateral hippocampus as compared to controls ($p < 0.05$, Figs. 9–10). Levels of *myo*-inositol

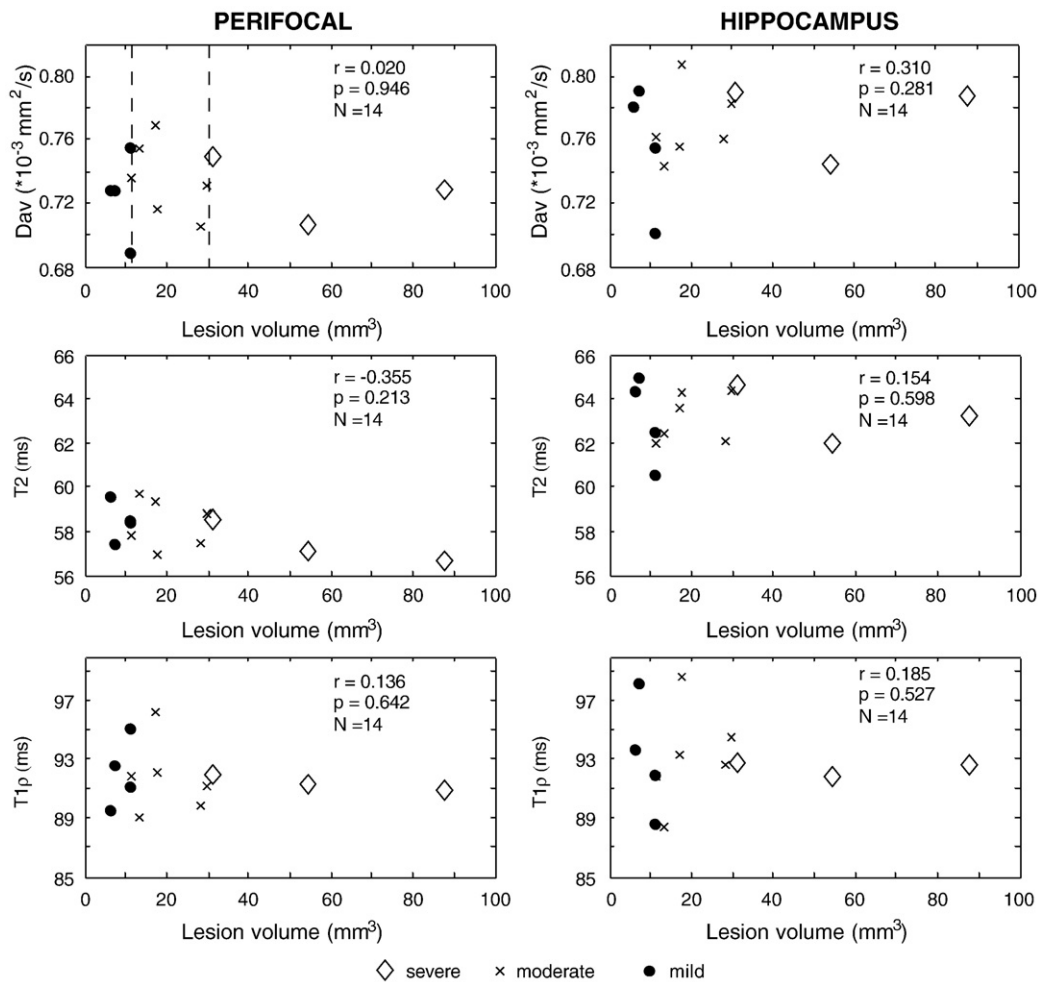


Fig. 8. The relationship between the volume of the focal lesion (x-axis) and the MRI changes (D_{av} , T_2 , $T_{1\rho}$) in the perifocal (left column) and the ipsilateral hippocampal (right column) areas at 23 d post-injury. The animals were divided into subgroups according to the cortical lesion volume on day 23: severe as diamonds, moderate as crosses, and mild as circles [the threshold volumes between mild and moderate (11 mm^3) and moderate and severe (30 mm^3) are indicated with dotted lines in the first panel]. Note that the size of the primary lesion did not correlate with the severity of alterations (evaluated by MRI) in the surrounding perifocal or hippocampal regions suggesting that the focal and more peripheral regions have different (independent) dynamics in the progression of tissue damage. Also, in several cases the animals with moderate lesions actually show more pathologic alterations in perifocal and ipsilateral hippocampal MRI contrast parameters than the animals with severe lesions.

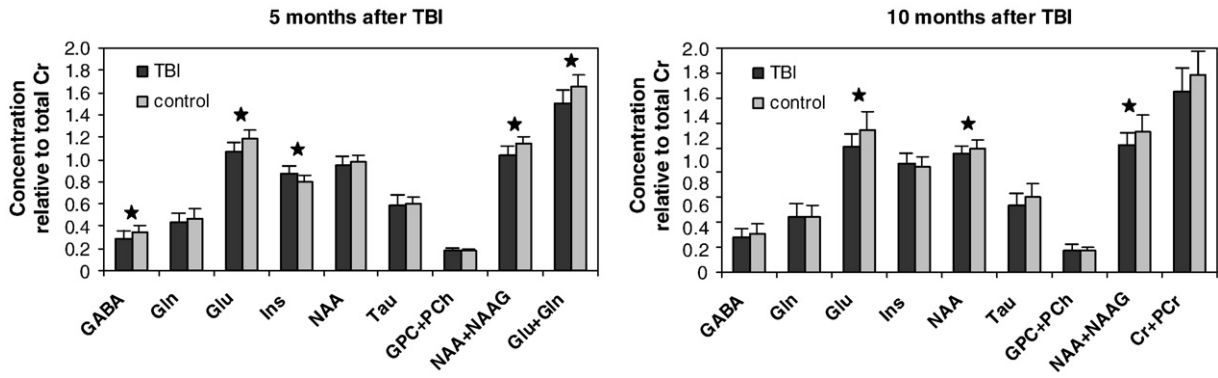


Fig. 9. Metabolic changes in the ipsilateral hippocampus at 5 and 10 months post-injury. Concentrations of different metabolites in MRS are shown as ratios relative to the creatine peak (Cr+PCr). Data are shown as mean±std. Statistical significances: * $p < 0.05$ (as compared to controls). Due to the hippocampal atrophy the amount of tissue in the voxel of TBI animals decreased and the use of absolute concentrations was not meaningful.

(Ins) were elevated ($p < 0.05$, Figs. 9–10). The further decrease of Glu was the only change from 5 months to 10 months ($p < 0.05$). No metabolic abnormalities were detected in the contralateral hippocampus.

Discussion

In order to understand the dynamics of brain damage after TBI, we performed quantitative MRI and MRS in a lateral fluid-percussion model of TBI in rat. We focused our analysis on the injured cortex, the perifocal area, and the hippocampus that are known to undergo histopathologic changes in this model (Hallam et al., 2004; Sato et al., 2001). In our 11 months follow-up study we have four major findings. First, brain damage after TBI progresses continually for up to 6 months. Second, D_{av} appeared to be the most sensitive measure for detecting both acute primary and secondary progressive damage. Third, the severity and dynamics of progression of injury varied substantially between the focal lesion area, adjacent perifocal area, and remote areas including the ipsilateral and contralateral hippocampus and the contralateral cortex. Importantly, temporal profiles of $T_{1\rho}$ and D_{av}

differentiated the regions with risk of delayed secondary damage from those of continuously progressing damage or from intact areas. Fourth, we describe the chronic hippocampal metabolic changes in this rat model providing the longest follow-up and the most detailed multiparametric MRI and MRS analysis of experimental TBI to date.

Early post-injury MRI shows a different temporal profile of alterations in the focal lesion and surrounding tissue differentiating regions with unpreventable or potentially preventable pathological processes

TBI causes both primary and secondary damage to the brain. The primary damage is caused by the impact itself, and it initiates ionic, molecular, and cellular alterations within seconds (Dietrich et al., 1994; McIntosh 1994; Rink et al., 1995) followed by immediate cytotoxic and later vasogenic oedema (Faden et al., 1989; Katayama et al., 1990). The primary cortical lesion was visually detectable in T_2 -weighted signal intensity images in a majority of animals already at 3 h post-injury, and in the quantitative analysis relaxation time $T_{1\rho}$ was elevated indicating increasing water content. D_{av} is known to transiently decrease during the cytotoxic edema (i.e. depolarization of

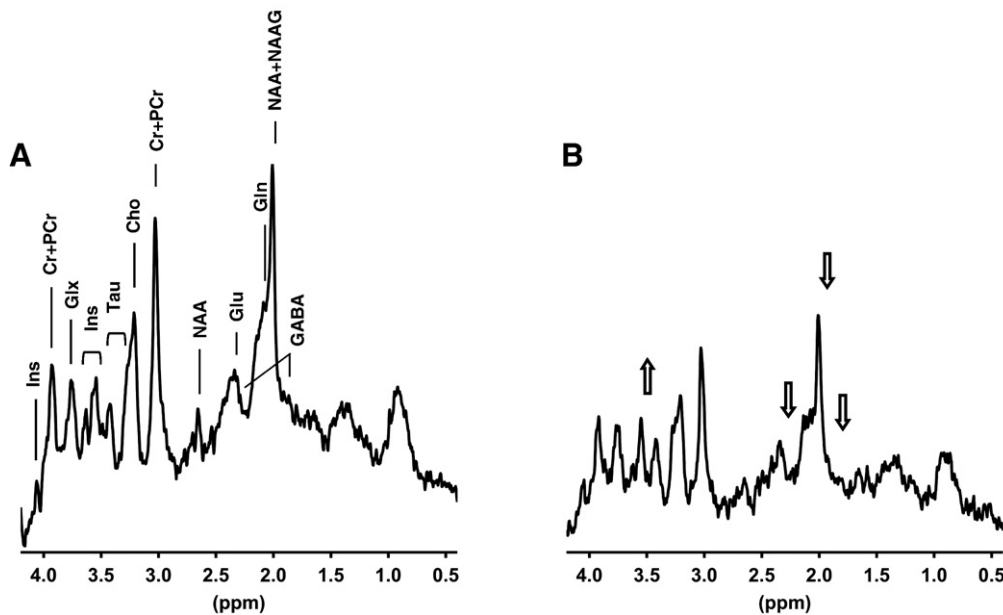


Fig. 10. A representative *in vivo* ^1H NMR spectrum of the ipsilateral hippocampus in a sham-operated rat (A) and a TBI rat (B) 5 months after the induction of TBI. LC model analysis was performed in the spectral region of 0.4 to 4.2 ppm and the spectra are shown with 4 Hz Gaussian line broadening. At 5 months post TBI, we found decreased relative concentrations (relative to Cr+PCr) of GABA, Glu, NAAG, NAA+NAAG and Glu+Gln and increased Ins as compared to controls ($p < 0.05$, open arrows in B, see Fig. 9. for more details). Due to the hippocampal atrophy the amount of tissue in the voxel of TBI animals decreased leading to overall reduction of metabolite peaks in B.

cells leading to intracellular swelling, which hinders water movement) (Moseley et al., 1990), however, in the primary lesion area the destruction of cellular structures restraining water diffusion was extremely fast leading to increased rather than decreased diffusion values in most of the animals already at 3 h post-injury. Importantly, characteristic of the primary lesion was that all T_2 , $T_{1\rho}$ and D_{av} were evidently increased at day 3 post-TBI and even more drastically elevated at day 9. The fact that all three measured parameters were so highly increased indicates a massive increase of the extracellular water content of the tissue, increasing amount of so called free water (that is, water molecules lacking interactions with surrounding macromolecules) reflecting the progressive loss of proteins in extracellular matrix together with cellular degeneration, and increased mobility of water molecules, which is another sign of degrading cytoarchitectural structures (Bramlett et al., 1997; Pierce et al., 1998; Smith et al., 1997).

In the perifocal area, in the ipsilateral hippocampus and to a lesser extent in the contralateral hippocampus, the tissue damage caused by primary impact was substantially milder as compared to the primary lesion site. In these regions the magnitude and also the pattern of MRI changes was very different from that in the primary lesion area. D_{av} showed a sharp decrease at 3 h post-injury and then returned to control level by 9 d post-injury, indicating cytotoxic edema at 3 h and its resolution thereafter. The diffusion drop was relatively small (7%) suggesting that only a subpopulation of the cells suffered from impact, which is in line with previous histologic studies (Cortez et al., 1989). T_2 and $T_{1\rho}$ increased at 3 d post-injury returning towards control level by 9 d post-injury, most likely reflecting the transient process of vasogenic edema, since both of these relaxation parameters are sensitive to net accumulation of water. Taken together, during the first 9 d post-injury we found a different temporal pattern in various MRI parameters in the primary lesion area and in areas that will later on undergo progressive secondary damage. This suggests that multi-parametric MRI analysis at an early post-injury phase can be a useful tool for identification of target regions for therapeutic interventions aiming at preventing delayed damage.

Secondary increase in D_{av} , T_2 and $T_{1\rho}$ during the first months post-injury implies the development of delayed injury in initially mildly affected regions

The secondary injury is composed of a series of biochemical, molecular and structural alterations that can be selective to cell types and brain regions (Conti et al., 1998; Hallam et al., 2004; Raghupathi et al., 2002; Rink et al., 1995; Sato et al., 2001). So far, *in vivo* detection of the progression of the damage with MRI has typically covered only the first 2 or 3 weeks post-injury showing hyperintense lesion in T_2 weighted images and increased cortical and hippocampal diffusion (Albensi et al., 2000; Van Putten et al., 2005; Vink et al., 2001). The only MRI study with a 3-month follow-up showed enlarged ventricles, cisterns and that the necrotic tissue in the primary contusion site was absorbed and replaced by cerebrospinal fluid (Iwamoto et al., 1997).

Here we show that the volume of the primary focal lesion as assessed in T_2 weighted images continued to progress for 3 months post-injury and tended to increase even thereafter. Our quantitative MRI analysis confirmed this observation by showing that the abnormal increase of all contrast parameters at the primary cortical lesion site progresses substantially for several months post-injury. At this time, the increased MRI contrast parameter values were close to that of CSF indicating almost complete decomposition of tissue. Histological studies have verified the robust cellular loss and cavity formation in the primary cortical contusion site during the first weeks post-injury (Bramlett et al., 1997; Pierce et al., 1998; Smith et al., 1997; Onyszchuk et al., 2008). Furthermore, we found a decrease of the volume of the ipsilateral hippocampus in the chronic stage, which is consistent with the previous histology studies showing hippocampal

neurodegeneration, and with the behavioural studies showing impaired hippocampal function after TBI (Pierce et al., 1998; Thompson et al., 2006).

As compared to the primary lesion, the adjacent perifocal area (*i.e.* the perilesional cortex), the remaining ipsilateral hippocampus and the contralateral hippocampus, had a very different temporal development of the secondary MRI alterations. In all these regions quantitative D_{av} , T_2 and $T_{1\rho}$ showed a delayed increase starting on the third week after TBI and continuing steadily for the first 3 months post-injury. Our MRI follow-up data are in line with the previous cross-sectional histological studies demonstrating ongoing pathology for up to 1 year, including chronic inflammation, neurodegeneration, and axonal injury (Bramlett et al., 1997; Lenzlinger et al., 2001; Morganti-Kossmann et al., 2002; Philips et al., 2001; Pierce et al., 1998; Smith et al., 1997; Soares et al., 1995; Toulmond and Rothwell 1995). Importantly however, the observed changes in MRI are showing the net effect of several progressive biological processes, both degenerative and regenerative. The fact that the observed changes do not seem to progress further after a few months can be due to the complexity of the underlying physiology and due to the complexity of how the physiological changes and the molecular interactions affect different MRI parameters. For example, in the animal model of mild TBI a partial recovery of average diffusion is reported 21 d post-injury even though other parameters remain on pathological levels (Henninger et al., 2007).

Relaxation is influenced by complex interactions of water with macromolecular pool. It has been suggested that $T_{1\rho}$ relaxation is specifically sensitive to slowly tumbling macromolecules as relaxation takes place in the effective magnetic field determined by RF pulses (Grohn et al., 2000; Makela et al., 2001; Sepponen et al., 1985). This may explain the more pronounced increase in $T_{1\rho}$ than in T_2 in the subacute phase (first 2 weeks post-injury) when destructive intracellular processes associated with delayed cell death have been launched.

MRS provides additional data about the molecular events during the chronic post-injury phase

In the present study the *in vivo* MRS data were evaluated as relative to Cr+PCr peak, that is a marker of overall cellular density, since there was evident atrophy of the hippocampus within the spectroscopy voxel in TBI animals. Our results showed several metabolic abnormalities in chronic TBI animals in the hippocampus ipsilateral to the impact site. Decreased NAA+NAAG is generally associated with decreased neuronal number, increased Ins with inflammation/gliosis, and decreased GABA with loss of inhibitory tone. All these observations are in line with previous cellular studies in the post-injury hippocampus showing neuronal loss (Pierce et al., 1998; Smith et al., 1997), inflammation (Lenzlinger et al., 2001; Philips et al., 2001; Soares et al., 1995) and alterations in GABA-mediated inhibition: (Reeves et al., 1997; Santhakumar et al., 2001). Previous MRS studies of the perifocal area reported decreased levels of Cr+PCr, NAA, and Glu at 28 d post-injury (Dube et al., 2001; Schuhmann et al., 2003). These studies suggest that tissue damage in the hippocampus and pericontusional cortex may share similarities in their MRS signature. Importantly, the metabolic changes found here resemble the metabolic changes found in TBI patients (Ashwal et al., 2004; Shutter et al., 2006), further validating the translational value of data obtained from the present animal model of TBI to the clinic.

Conclusions

Our results distinguish two different patterns of brain tissue alterations in the aftermath of TBI based on the temporal fluctuation of quantitative MRI parameters. First, at the primary lesion area with drastic irreversible pathologic MRI alterations start at 3 h–3 d post-injury and continue to progress steadily for months. Second, in more

mildly affected perifocal and hippocampal regions the alteration in T_2 , $T_{1\rho}$, D_{av} at 3 h–3 d post-injury normalize within the first 3–23 d, and then show a progressive increase for several weeks. Interestingly, the severity of damage in the perifocal and hippocampal areas appeared independent of the focal lesion volume at subacute phase suggesting the insufficiency of using solely the lesion volume as an indicator of injury severity. Our data show that the temporal profile of MRI parameters can indicate the regions that will develop secondary damage. Based on the observations of this study together with the existing literature of secondary damage in traumatic brain injury we tentatively suggest that the ‘tissue at risk’ could be identified as having 5–10% increased diffusion and T_2 (or $T_{1\rho}$, which appears to be slightly more sensitive than T_2) 23 d–3 months post-injury when oedema has been reabsorbed and secondary injury cascades have been initiated. Importantly, most of the MRI techniques used here can be readily translated for clinical applications. Only the use of $T_{1\rho}$ techniques is somewhat restricted with high specific absorption rate (SAR) caused by long RF pulses, but they have already been used in a few feasibility studies in humans (Duvvuri et al., 2001; Grohn et al., 2005; Michaeli et al., 2006). The information provided by this study is valuable for the targeting and timing of interventions in studies aiming to alleviate or even reverse the molecular and/or cellular cascades causing the delayed injury.

Acknowledgments

This work was supported by the Academy of Finland, the Emil Aaltonen Foundation, the Sigrid Juselius Foundation, CURE (Citizens United for Research for Epilepsy), the Finnish Epilepsy Research Foundation, and the Finnish Cultural Foundation. We thank Mrs. Maarit Pulkkinen, Mr. Jarmo Hartikainen, Mrs. Merja Lukkari, and Jari Nissinen, Ph.D., for technical assistance, Nick Hayward, M.Sc., for revising the language of the manuscript, and Ivan Tkáč providing the short echo time STEAM pulse sequence.

References

- Albensi, B.C., Knobloch, S.M., Chew, B.G., O'Reilly, M.P., Faden, A.I., Pekar, J.J., 2000. Diffusion and high resolution MRI of traumatic brain injury in rats: time course and correlation with histology. *Exp. Neurol.* 162, 61–72.
- Ashwal, S., Holshouser, B., Tong, K., Serna, T., Osterdock, R., Gross, M., Kido, D., 2004. Proton spectroscopy detected myoinositol in children with traumatic brain injury. *Pediatr. Res.* 56, 630–638.
- Berry, I., Moseley, M., Germano, I.M., Ishige, N., Nishimura, M.C., Bartkowski, H.M., Pitts, L.H., Brant-Zawadzki, M., 1986. Combined magnetic resonance imaging and spectroscopy in experimental regional injury of the brain. ischemia and impact trauma. *Acta Radiol. Suppl.* 369, 338–349.
- Bramlett, H.M., Kraydieh, S., Green, E.J., Dietrich, W.D., 1997. Temporal and regional patterns of axonal damage following traumatic brain injury: a beta-amyloid precursor protein immunocytochemical study in rats. *J. Neuropathol. Exp. Neurol.* 56, 1132–1141.
- Choi, C.B., Kim, H.Y., Han, D.Y., Kang, Y.W., Han, Y.M., Jeun, S.S., Choe, B.Y., 2005. In vivo 1H MR spectroscopic findings in traumatic contusion of ICR mouse brain induced by fluid percussion injury. *Eur. J. Radiol.* 55, 96–101.
- Conti, A.C., Raghupathi, R., Trojanowski, J.Q., McIntosh, T.K., 1998. Experimental brain injury induces regionally distinct apoptosis during the acute and delayed post-traumatic period. *J. Neurosci.* 18, 5663–5672.
- Cortez, S.C., McIntosh, T.K., Noble, L.J., 1989. Experimental fluid percussion brain injury: vascular disruption and neuronal and glial alterations. *Brain Res.* 482, 271–282.
- Dietrich, W.D., Alonso, O., Halley, M., 1994. Early microvascular and neuronal consequences of traumatic brain injury: a light and electron microscopic study in rats. *J. Neurotrauma* 11, 289–301.
- Dube, C., Boyet, S., Marescaux, C., Nehlig, A., 2001. Relationship between neuronal loss and interictal glucose metabolism during the chronic phase of the lithium-pilocarpine model of epilepsy in the immature and adult rat. *Exp. Neurol.* 167, 227–241.
- Dubreuil, C.I., Marklund, N., Deschamps, K., McIntosh, T.K., McKerracher, L., 2006. Activation of rho after traumatic brain injury and seizure in rats. *Exp. Neurol.* 198, 361–369.
- Duvvuri, U., Charagundla, S.R., Kudchodkar, S.B., Kaufman, J.H., Kneeland, J.B., Rizi, R., Leigh, J.S., Reddy, R., 2001. Human knee: in vivo T1(rho)-weighted MR imaging at 1.5 T—preliminary experience. *Radiology* 220, 822–826.
- Faden, A.I., Demediuk, P., Panter, S.S., Vink, R., 1989. The role of excitatory amino acids and NMDA receptors in traumatic brain injury. *Science* 244, 798–800.
- Grohn, O.H.J., Kettunen, M.I., Makela, H.I., Penttonen, M., Pitkanen, A., Lukkari, J.A., Kauppinen, R.A., 2000. Early detection of irreversible cerebral ischemia in the rat using dispersion of the magnetic resonance imaging relaxation time, T1rho. *J. Cereb. Blood Flow Metab.* 20, 1457–1466.
- Grohn, H.I., Michaeli, S., Garwood, M., Kauppinen, R.A., Grohn, O.H., 2005. Quantitative T1(rho) and adiabatic carr-purcell T2 magnetic resonance imaging of human occipital lobe at 4 T. *Magn. Reson. Med.* 54, 14–19.
- Gruetter, R., 1993. Automatic, localized in vivo adjustment of all first- and second-order shim coils. *Magn. Reson. Med.* 29, 804–811.
- Hallam, T.M., Floyd, C.L., Folkerts, M.M., Lee, L.L., Gong, Q.Z., Lyeth, B.G., Muizelaar, J.P., Berman, R.F., 2004. Comparison of behavioral deficits and acute neuronal degeneration in rat lateral fluid percussion and weight-drop brain injury models. *J. Neurotrauma* 21, 521–539.
- Henninger, N., Sicard, K.M., Li, Z., Kulkarni, P., Dutzmann, S., Urbaneck, C., Schwab, S., Fisher, M., 2007. Differential recovery of behavioral status and brain function assessed with functional magnetic resonance imaging after mild traumatic brain injury in the rat. *Crit. Care Med.* 35, 2607–2614.
- Iwamoto, Y., Yamaki, T., Murakami, N., Umeda, M., Tanaka, C., Higuchi, T., Aoki, I., Naruse, S., Ueda, S., 1997. Investigation of morphological change of lateral and midline fluid percussion injury in rats, using magnetic resonance imaging. *Neurosurgery* 40, 163–167.
- Karhunen, H., Jolkkonen, J., Sivenius, J., Pitkanen, A., 2005. Epileptogenesis after experimental focal cerebral ischemia. *Neurochem. Res.* 30, 1529–1542.
- Katayama, Y., Becker, D.P., Tamura, T., Hovda, D.A., 1990. Massive increases in extracellular potassium and the indiscriminate release of glutamate following concussive brain injury. *J. Neurosurg.* 73, 889–900.
- Kharatishvili, I., Nissinen, J.P., McIntosh, T.K., Pitkanen, A., 2006. A model of posttraumatic epilepsy induced by lateral fluid-percussion brain injury in rats. *Neuroscience* 140, 685–697.
- Kharatishvili, I., Immonen, R., Grohn, O., Pitkanen, A., 2007. Quantitative diffusion MRI of hippocampus as a surrogate marker for post-traumatic epileptogenesis. *Brain* 130, 3155–3168.
- Lenzinger, P.M., Morganti-Kossmann, M.C., Laurer, H.L., McIntosh, T.K., 2001. The duality of the inflammatory response to traumatic brain injury. *Mol. Neurobiol.* 24, 169–181.
- Leon-Carrion, J., Dominguez-Morales Mdel, R., Barroso y Martin, J.M., Murillo-Cabezas, F., 2005. Epidemiology of traumatic brain injury and subarachnoid hemorrhage. *Pituitary* 8, 197–202.
- Makela, H.I., Grohn, O.H., Kettunen, M.I., Kauppinen, R.A., 2001. Proton exchange as a relaxation mechanism for T1 in the rotating frame in native and immobilized protein solutions. *Biochem. Biophys. Res. Commun.* 289, 813–818.
- McIntosh, T.K., 1994. Neurochemical sequelae of traumatic brain injury: therapeutic implications. *Cerebrovasc. Brain Metab. Rev.* 6, 109–162.
- McIntosh, T.K., Vink, R., Noble, L., Yamakami, I., Feryak, S., Soares, H., Faden, A.L., 1989. Traumatic brain injury in the rat: characterization of a lateral fluid-percussion model. *Neuroscience* 28, 233–244.
- Michaeli, S., Sorce, D.J., Springer Jr, C.S., Ugurbil, K., Garwood, M., 2006. T1rho MRI contrast in the human brain: modulation of the longitudinal rotating frame relaxation shutter-speed during an adiabatic RF pulse. *J. Magn. Reson.* 181, 135–147.
- Morganti-Kossmann, M.C., Rancan, M., Stahel, P.F., Kossmann, T., 2002. Inflammatory response in acute traumatic brain injury: a double-edged sword. *Curr. Opin. Crit. Care* 8, 101–105.
- Moseley, M.E., Kucharczyk, J., Mintorovitch, J., Cohen, Y., Kurhanewicz, J., Derugin, N., Asgari, H., Norman, D., 1990. Diffusion-weighted MR imaging of acute stroke: correlation with T2-weighted and magnetic susceptibility-enhanced MR imaging in cats. *AJNR Am. J. Neuroradiol.* 11, 423–429.
- Obenaus, A., Robbins, M., Blanco, G., Galloway, N.R., Snissarenko, E., Gillard, E., Lee, S., Curras-Collazo, M., 2007. Multi-modal magnetic resonance imaging alterations in two rat models of mild neurotrauma. *J. Neurotrauma* 24, 1147–1160.
- Onyszchuk, G., Al-Hafez, B., He, Y.Y., Bilgen, M., Berman, N.E., Brooks, W.M., 2007. A mouse model of sensorimotor controlled cortical impact: characterization using longitudinal magnetic resonance imaging, behavioral assessments and histology. *J. Neurosci. Methods* 160, 187–196.
- Onyszchuk, G., He, Y.Y., Berman, N.E., Brooks, W.M., 2008. Detrimental effects of aging on outcome from traumatic brain injury: a behavioral, magnetic resonance imaging, and histological study in mice. *J. Neurotrauma* 25, 153–171.
- Philips, M.F., Mattiasson, G., Wieloch, T., Bjorklund, A., Johansson, B.B., Tomasevic, G., Martinez-Serrano, A., Lenzinger, P.M., Sinson, G., Grady, M.S., et al., 2001. Neuroprotective and behavioral efficacy of nerve growth factor-transfected hippocampal progenitor cell transplants after experimental traumatic brain injury. *J. Neurosurg.* 94, 765–774.
- Paxinos, G., Watson, C., 1986. *The Rat Brain in Stereotaxic Coordinates*. Academic Press, New York.
- Pierce, J.E., Smith, D.H., Trojanowski, J.Q., McIntosh, T.K., 1998. Enduring cognitive, neurobehavioral and histopathological changes persist for up to one year following severe experimental brain injury in rats. *Neuroscience* 87, 359–369.
- Raghupathi, R., Conti, A.C., Graham, D.I., Krajewski, S., Reed, J.C., Grady, M.S., Trojanowski, J.Q., McIntosh, T.K., 2002. Mild traumatic brain injury induces apoptotic cell death in the cortex that is preceded by decreases in cellular bcl-2 immunoreactivity. *Neuroscience* 110, 605–616.
- Reeves, T.M., Lyeth, B.G., Phillips, L.L., Hamm, R.J., Povlishock, J.T., 1997. The effects of traumatic brain injury on inhibition in the hippocampus and dentate gyrus. *Brain Res.* 757, 119–132.
- Rink, A., Fung, K.M., Trojanowski, J.Q., Lee, V.M., Neugebauer, E., McIntosh, T.K., 1995. Evidence of apoptotic cell death after experimental traumatic brain injury in the rat. *Am. J. Pathol.* 147, 1575–1583.

- Santhakumar, V., Ratzliff, A.D., Jeng, J., Toth, Z., Soltesz, I., 2001. Long-term hyperexcitability in the hippocampus after experimental head trauma. *Ann. Neurol.* 50, 708–717.
- Sato, M., Chang, E., Igarashi, T., Noble, L.J., 2001. Neuronal injury and loss after traumatic brain injury: Time course and regional variability. *Brain Res.* 917, 45–54.
- Schuhmann, M.U., Stiller, D., Skardelly, M., Thomas, S., Samii, M., Brinker, T., 2002. Long-time in-vivo metabolic monitoring following experimental brain contusion using proton magnetic resonance spectroscopy. *Acta Neurochir. Suppl.* 81, 209–212.
- Schuhmann, M.U., Stiller, D., Skardelly, M., Bernarding, J., Klinge, P.M., Samii, A., Samii, M., Brinker, T., 2003. Metabolic changes in the vicinity of brain contusions: a proton magnetic resonance spectroscopy and histology study. *J. Neurotrauma* 20, 725–743.
- Sepponen, R.E., Pohjonen, J.A., Sipponen, J.T., Tantt, J.L., 1985. A method for T1 rho imaging. *J. Comput. Assist. Tomogr.* 9, 1007–1011.
- Shutter, L., Tong, K.A., Lee, A., Holshouser, B.A., 2006. Prognostic role of proton magnetic resonance spectroscopy in acute traumatic brain injury. *J. Head Trauma Rehabil.* 21, 334–349.
- Smith, D.H., Chen, X.H., Pierce, J.E., Wolf, J.A., Trojanowski, J.Q., Graham, D.I., McIntosh, T.K., 1997. Progressive atrophy and neuron death for one year following brain trauma in the rat. *J. Neurotrauma* 14, 715–727.
- Soares, H.D., Hicks, R.R., Smith, D., McIntosh, T.K., 1995. Inflammatory leukocytic recruitment and diffuse neuronal degeneration are separate pathological processes resulting from traumatic brain injury. *J. Neurosci.* 15, 8223–8233.
- Thompson, H.J., Lifshitz, J., Marklund, N., Grady, M.S., Graham, D.I., Hovda, D.A., McIntosh, T.K., 2005. Lateral fluid percussion brain injury: a 15-year review and evaluation. *J. Neurotrauma* 22, 42–75.
- Thompson, H.J., LeBold, D.G., Marklund, N., Morales, D.M., Hagner, A.P., McIntosh, T.K., 2006. Cognitive evaluation of traumatically brain-injured rats using serial testing in the morris water maze. *Restor. Neurol. Neurosci.* 24, 109–114.
- Tkac, I., Starcuk, Z., Choi, I.Y., Gruetter, R., 1999. In vivo ¹H NMR spectroscopy of rat brain at 1 ms echo time. *Magn. Reson. Med.* 41, 649–656.
- Toulmond, S., Rothwell, N.J., 1995. Interleukin-1 receptor antagonist inhibits neuronal damage caused by fluid percussion injury in the rat. *Brain Res.* 671, 261–266.
- Van Putten, H.P., Bouwhuis, M.G., Muizelaar, J.P., Lyeth, B.G., Berman, R.F., 2005. Diffusion-weighted imaging of edema following traumatic brain injury in rats: effects of secondary hypoxia. *J. Neurotrauma* 22, 857–872.
- Vink, R., Mullins, P.G., Temple, M.D., Bao, W., Faden, A.I., 2001. Small shifts in craniotomy position in the lateral fluid percussion injury model are associated with differential lesion development. *J. Neurotrauma* 18, 839–847.